Paper B

Investigation of Turbulence Injection Methods in Compressible Flow Solvers in Large Eddy Simulation

M. Carlsson, L. Davidson, S.H. Peng, and S. Arvidson. "Investigation of Turbulence Injection Methods in Compressible Flow Solvers in Large Eddy Simulation". ***2022 AIAA SciTech Forum.*** **Jan. 2022.** DOI: 10.2514/6.2022-0483

Investigation of Turbulence Injection Methods in Large Eddy Simulation using a Compressible Flow Solver

Magnus Carlsson *[1], Lars Davidson †[1], Shia-Hui Peng ‡ §[1,2], and Sebastian Arvidson ¶ ‖[1,3]
[1]*Division of Fluid Dynamics and Maritime Sciences, Chalmers University of Technology, SE-412 96, Gothenburg, SWEDEN*
[2]*Swedish Defence Research Agency, FOI, SE-16490 Stockholm, SWEDEN*
[3]*Propulsion Systems, Saab Aeronautics, SE-581 88, Linköping, SWEDEN*

Three different methods for imposing velocity fluctuations in a compressible finite-volume solver are evaluated for zonal hybrid RANS-LES applications using the SA-IDDES model. The first method is a volume source term derived from an expansion of the time discretization of the fluctuating velocity component, suitable for an unstructured solver. The second method stems from an expansion of the convective flux of the fluctuating velocity component normal to the flow direction. The third methods considers a combination of both aforementioned methods. Additionally, a commutation term is derived for the convection term in the SA turbulence model in order rapidly reduce the turbulent viscosity across the RANS-LES interface. Good agreement with reference data is obtained with the investigated interface methods for the evaluated flow cases, which includes the turbulent channel flow and the zero-pressure-gradient boundary layer flow.

I. Introduction

Computational Fluid Dynamics (CFD) is a powerful tool for the aeronautical industry in predicting complex turbulent flows. Reynolds-averaged Navier–Stokes (RANS) is an industry standard computational technique, where temporal and spatial turbulent length scales are completely modeled. The method have been proven to effectively estimate turbulent flows in attached boundary layers at an affordable computational cost. However, RANS based methods are rather inaccurate in predicting turbulent flows around bluff bodies that produce massively separated flow regions. Scale-resolving methods such as Large-Eddy-Simulation (LES), where the turbulent scales are partly resolved have been shown to be much more accurate than RANS in estimating separated flow regions. However, LES is much more computationally demanding than RANS and is expected to remain unfeasible for complex engineering computations in the foreseeable future.

Hybrid RANS-LES modeling (HRLM) is a computational technique considered to be more accurate than RANS and computationally more affordable than LES for the aeronautical industry. The key feature of HRLM is the RANS-type behavior inside the near wall boundary layer coupled with a LES-type behavior further away from the wall. The most commonly used HRLM methods are based on Detached Eddy Simulation (DES) by Spalart et. al [1] and extended by boundary-layer shielding, e.g. Delayed DES (DDES), which is considered to be the most mature for industrial use. A wide variety of additional methods exist such as Improved DDES (IDDES) [2], HYB0 [3, 4], SAS and PANS (e.g. [5]).

In zonal RANS-LES approaches, zonal scale-resolving simulations are enabled using a LES mode embedded in an overall RANS computation. The embedded coupling often leads to the so-called "grey-area" problem, which delays the development of LES-resolved turbulence in association to the RANS-modeling over the RANS-LES interface. As a result, the accuracy of scale-resolving simulation in the focusing LES region may become significantly degraded or might even generate nonphysical predictions. In order to have effective transition between the RANS mode and the LES mode, Synthetic Turbulence (ST) have been often employed at the RANS-LES interface. The synthetic turbulent fluctuations are often superimposed on the mean flow over the RANS-LES interface to mitigate the grey-area problem.

Common ST methods are usually based on Fourier reconstruction techniques [6–8], where Fourier series is used as a mean to introduce spatial correlation. Time correlation can be introduced through imposing a time filter [7] or

*PhD. student, Division of Fluid Dynamics and Maritime Sciences, Chalmers University of Technology.
†Professor, Division of Fluid Dynamics and Maritime Sciences, Chalmers University of Technology.
‡Professor, Division of Fluid Dynamics and Maritime Sciences, Chalmers University of Technology.
§Research Director, Division of Defense Technology, FOI. peng@foi.se, AIAA associate fellow.
¶PhD. Systems Engineer, Propulsion Aerodynamics and Performance, Saab Aeronautics
‖PhD. Visiting Researcher, Department of Mechanics and Maritime Sciences, Chalmers University of Technology.

using a modified position vector [8], where time correlation is imposed in the streamwise direction of the flow using mean flow quantities. An alternative approach is the Synthetic Eddy methods (SEM) [9, 10], where the flow field is superimposed by virtual vortical structures. These vortical structures or eddies are randomly generated and convected through a fictional domain giving both spatial and temporal correlation to the fluctuations, which are allowed to induce perturbations to cells in their neighbourhood. Further improvement was made to the original SEM, where it was extended to give a divergence-free (DF-SEM) [11] fluctuating velocity field.

For grey-area mitigation in zonal hybrid RANS-LES computations, different methods to inject the artificial velocity fields into the flow domain have been proposed. In scale-resolving simulations, for example in LES, a Dirichlet boundary condition can be readily used for the velocities by directly imposing the fluctuations at the inlet boundary. In the work by Mathey [12] and Davidson [13], they imposed the fluctuations as an embedded approach where virtual fluxes are added to the momentum equations. The virtual fluxes are derived from an expansion of the convective flux term and were added to an interface plane between a RANS and a LES region. However, these studies were using the incompressible flow equations. Other approaches are based on the expansion of the time-derivative term, where in the works by Schmidt et al. [14] and Probst [15], they investigated a volumetric source term to impose the fluctuations. The expansion is based on the time derivative of the momentum equations, the fluctuations in the continuity and total energy equations are assumed to be small and are neglected.

In order to provide a rapid development of the turbulence-resolving LES flow, excess modeled turbulence (i.e. turbulent viscosity) need to be reduced across the RANS-LES interface. If not, the resolved turbulence imposed by the ST methods might be dampened and further delay the development of resolved turbulence. Hamba [16] identified a commutation error, owing to the non-commutivity of the spatial derivative and the filter applied in RANS and LES, at the RANS-LES interface. It was found that the commutation error can be large across the RANS-LES interface and should be considered. Following the work by Hamba, Davidson [17] and Arvidson et al. [18] explored the combination of the commutation term with synthetic fluctuations at interfaces in hybrid RANS-LES simulations, with the aim to reduce the turbulent viscosity across the RANS-LES interface. Commutation terms were derived for the k and ω equations used for the hybrid RANS-LES model and successively applied to embedded hybrid simulations, such as turbulent channel flow, zero-pressure-gradient boundary layer and mixing boundary layers.

In this work, we further explore the effects of the aforementioned injection methods using the Synthethic Turbulence Generator (STG) by Shur et al. [8]. A virtual flux term suitable for a compressible solver is derived and compared to the source term based on the time derivative. In order to provide a more complete description of the injected fluctuations, a combination of the two methods are evaluated. We apply the proposed methodology to embedded LES simulations of turbulent channel flow and boundary layer flow, using the SA-IDDES hybrid RANS-LES turbulence model [2, 19]. Hence, a commutation term suitable for the SA-model is also derived and evaluated. The efficiency and performance of the proposed methodology are evaluated and implemented into a compressible flow solver, M-Edge [20, 21].

The paper is organized as follows. In Sections II and III the synthetic turbulence methods and turbulence models used in this paper are outlined. The numerical method, injection methods and the commutation term are presented in Section IV. In Section V, the performance of these methods are assessed by their capabilities of mitigating grey area, by comparing the resolved turbulent statistics and the skin friction coefficient. Finally, some conclusions are made with a proposed continuation of the work in Section VI.

II. Synthetic Turbulence Method

The synthetic turbulence method considered in this paper is the Synthetic Turbulence Generator (STG) by Shur et al. [8]. The velocity fluctuations are computed by superimposing N Fourier modes:

$$\mathbf{v}'(\mathbf{r},t) = \sqrt{6}\sum_{k=1}^{N}\sqrt{q^n}\left[\boldsymbol{\sigma}^n\cos(k^n\mathbf{d}^n\cdot\mathbf{r}'+\phi^n)\right] \tag{1}$$

Here, the fluctuating field $\mathbf{v}'$ is computed from random quantities (mode direction vectors $\mathbf{d}^n$, $\boldsymbol{\sigma}^n\cdot\mathbf{d}^n=0$ and mode phase ϕ^n), and statistical quantities such as the wave number amplitude k^n, which is computed from upstream RANS statistics and grid metrics. A modified von Karman spectrum is used to compute the mode amplitude q^n. An important note is that the random numbers used in (1) is only computed once. Unlike in [7], where a time-filter is introduced to impose a temporal correlation between the fluctuations, a modified position vector $\mathbf{r}'$ is introduced and linked with the actual quantities $\mathbf{x}$ and t using Taylor's frozen velocity hypothesis [8].

The velocity fluctuations $\mathbf{v}'(\mathbf{r},t)$ in (1) satisfies the restrictions $\langle v_i'\rangle=0$ and $\langle v_i'v_j'\rangle=\delta_{ij}$, where $\langle\cdot\rangle$ denotes time averaging. In order to impose the correct Reynolds stress statistics at the interface, the actual fluctuations $\mathbf{u}'(\mathbf{x},t)$ are

computed from

$$\mathbf{u}'(\mathbf{x},t) = a_{ij}\mathbf{v}'(\mathbf{r},t) \tag{2}$$

where a_{ij} is the Cholesky-decomposed Reynolds stress tensor:

$$a_{ij} = \begin{bmatrix} \sqrt{R_{11}} & 0 & 0 \\ R_{21}/a_{11} & \sqrt{R_{22}-a_{21}^2} & 0 \\ R_{31}/a_{11} & (R_{32}-a_{21}a_{31})/a_{22} & \sqrt{R_{33}-a_{31}^2-a_{32}^2} \end{bmatrix} \tag{3}$$

a_{ij} determines the magnitude of the velocity fluctuation as a function of the estimated Reynolds stresses $R_{ij} =< u_i' u_j' >$, taken from upstream RANS modeled stresses in the hybrid RANS-LES simulation.

III. Turbulence Modeling

For the simulation of wall bounded flows with synthetic turbulence (ST) injection, the Improved Delayed DES (IDDES) [2] based on the SA-model [19] is employed. The IDDES blends two branches, the DDES-like branch which should become active only when the inflow conditions do not have any turbulent content, and the WMLES-like branch intended to be active only when the inflow conditions used in the simulation are unsteady and impose some turbulent content and if the grid is fine enough to resolve boundary-layer dominant eddies. The blending function between the RANS mode and the LES mode reads:

$$l_{hyb} = \tilde{f}_d(1+f_e)l_{RANS} + (1-\tilde{f}_d)l_{LES} \tag{4}$$

where l_{RANS} for the SA-model is the wall distance d. The SA-model can then work as a hybrid RANS-LES model by replacing the wall distance d by the hybrid length scale given by l_{hyb}. The LES length scale in (4) is given by

$$l_{LES} = C_{DES}\Psi\Delta, \quad \Delta = \min(\max[C_{dw}d, C_{dw}\Delta_{max}, \Delta_{min}], \Delta_{max}) \tag{5}$$

Here, $C_{DES} = 0.65$ and Ψ is a damping function [2]. In the edge-based solver (further outlined in Section IV), Δ_{max} and Δ_{min} in Eq. (5) are approximated as the maximum and minimum edge length of a dual-cell, respectively.

In an zonal approach, a RANS region upstream of the ST-injection interface can be enforced by setting the hybrid length scale to the RANS length scale of the underlying turbulence model, $l_{hyb} = l_{RANS}$. Then, further downstream of the interface Eq. (4) can be used without any modification. In this way, no assumptions are made about the downstream region. A schematic of a zonal approach is presented in Fig. 1.

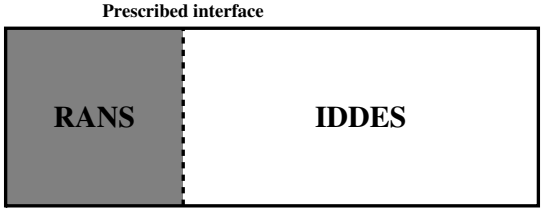

Fig. 1 Schematic of RANS and LES regions in zonal hybrid RANS-LES (embedded LES) with wall-normal RANS-LES interfaces indicated.

An alternative method is to modify the switching function f_{dt} [22]

$$\tilde{f}_d = \max(1-f_{dt}, f_B), \quad f_{dt} = 1-\tanh[(8r_{dt})^3] \tag{6}$$

where f_{dt} is set to 0 in the upstream RANS region, driving the length scale to $l_{hyb} = l_{RANS}$. Downstream of the interface the WMLES mode is enforced by setting $f_{dt} = 1$. This was necessary since without manual switch to WMLES mode, the large (RANS-level) eddy viscosity resulted in too strong damping of the injected fluctuations [22]. In Section IV.B, a method to reduce the upstream RANS-level eddy viscosity at the interface is presented, which does not require a manual switch to WMLES mode.

The turbulent stresses used in Eq. (3) needs to be approximated by the RANS-model. This can be achieved by the eddy viscosity assumption:

$$-\rho < u_i' u_j' >= 2\mu_t S_{ij} - \frac{2}{3}\rho k \delta_{ij} \tag{7}$$

The modeled kinetic energy k in Eq. (7) is usually not computed in the SA-model but at a RANS-LES interface where synthetic turbulence is to be generated by Eq. (1), non-zero normal stresses $< u_i' u_i' >$ have to be provided. The turbulent kinetic energy is estimated as [23]

$$k \approx \frac{\mu_t S}{\rho\sqrt{C_\mu}} \tag{8}$$

where $S = \sqrt{2S_{ij}S_{ij}}$ is the magnitude of the strain rate tensor. It is reported in [24] that the ratio between the Reynolds shear stress $- < u_1' u_2' >$ and the turbulent kinetic energy k is nearly the same for a wide range of flows, including boundary layers, wakes and mixing layers. This constant is fixed to 0.3 and Eq. (8) agrees well with this relationship for a zero pressure gradient boundary layer where $\sqrt{C_\mu} = 0.3$ and $S \approx - < u_1' u_2' >$. The reconstructed isotropic normal stresses are then evaluated as

$$< u'^2 >=< v'^2 >=< w'^2 >= \frac{2}{3}k \tag{9}$$

where k is computed according to Eq. (8). In order to take into account the turbulence anisotropy, a more realistic distribution of the normal shear stresses can be employed. The anisotropic Reynolds stress tensor can be computed by the Wallin and Johansson EARSM model [25], which requires the modeled kinetic energy k and specific dissipation ω at the interface. However, in the work by Wilcox [26], it is shown that in the case of a zero pressure gradient turbulent boundary layer (ZPG), the following expression provide a good approximations throughout the log layer and most of the defect layer:

$$< u'^2 >= \frac{4}{9}2k, \quad < v'^2 >= \frac{2}{9}2k, \quad < w'^2 >= \frac{3}{9}2k. \tag{10}$$

Equation (10) is only a slight modification to Eq. (9), where the spanwise stresses remain unaffected. The robustness and efficiency of Eq. (10) was further verified by Deck et al. [24] for the ZPG boundary layer in case hybrid RANS-LES, when used for reconstruction stresses from the SA-model in combination with synthetic turbulence (the ST model used in [24] was the SEM [10], but it uses the same expression as Eq. (3) for anisotropic stresses). In this paper, the anisotropic normal stresses given by Eq. (10) is used.

IV. Numerical Method

The flow solver used in this paper is the M-Edge code, which is an edge- and node-based Navier-Stokes flow solver applicable for both structured and unstructured grids [20, 27]. The compressible Navier-Stokes equations are discretized with a finite-volume approximation and is integrated in time using a 2nd-order backward difference scheme, together with a dual-time stepping methodology using an explicit low-storage multistage Runge-Kutta scheme accelerated by local-timestepping and full-approximation storage (FAS) multigrid [28]. The boundary conditions are based on a weak formulation in which a set of temporary flow variables are computed and used in the calculations of the boundary flux added to the residual. The residual is then used to update all unknown variables including the boundary values [21]. The viscous fluxes are discretized with a 2nd-order central scheme. The inviscid fluxes are based on the LD2 scheme, which combines a low-dissipative convection operator with a low-dispersive reconstruction of the face values [29]. The LD2-scheme was successfully applied to reduce the numerical dissipation and dispersion for fully developed turbulent channel flow and decaying homogenous isotropic turbulence [30].

A. Synthetic Turbulence Injection

The velocity fluctuations provided by the STG in Eq. (2) are injected by considering three different methods. A forcing region is defined at the RANS-LES interface, which is a plane perpendicular to the general flow direction, where cells that intersect this plane are identified by manual input. This is visualized in Fig. 1. The velocity fluctuations are then added to the flow solver using three different methods outlined below.

The first method represents the injected fluctuations by means of a flux [12] added to the momentum residuals

$$F_i = \rho S_n \left(u_n u_i' + u_n' u_i + u_n' u_i'\right) \tag{11}$$

where $u_n = u_i n_i$, $u'_n = u'_i n_i$, u'_i is taken from Eq. (2) and n_i denotes the unit vector normal to the interface S_n. The expression (11) is derived for an incompressible solver. The extension of Eq. (11) suitable for a compressible solver is straightforward. Consider a convective flux projected in the plane (n_x, n_y, n_z)

$$\vec{F}_c = S_n \begin{bmatrix} \rho V \\ \rho u V + n_x p \\ \rho v V + n_y p \\ \rho w V + n_z p \\ \rho H V \end{bmatrix} \tag{12}$$

where $V = n_x u + n_y v + n_z w$ is the projected normal velocity and $H = E + p/\rho = e + u_i u_i/2 + p/\rho$ is the total enthalpy. By letting $u_i \rightarrow \tilde{u}_i + u'_i$ in Eq. (12), where $\tilde{u}_i$ is the instantaneous velocity, and identifying all terms that contain a fluctuating part, an additional flux associated to the fluctuations is derived in the following form:

$$\vec{F}_c^{\text{virt}} = S_n \begin{bmatrix} \rho V' \\ \rho(\tilde{u}V' + u'(\tilde{V} + V')) \\ \rho(\tilde{v}V' + v'(\tilde{V} + V')) \\ \rho(\tilde{w}V' + w'(\tilde{V} + V')) \\ \rho H V' + \rho(\frac{1}{2}(2\tilde{u}_i u'_i + u'_i u'_i))(\tilde{V} + V') \end{bmatrix} \tag{13}$$

where $V' = n_x u' + n_y v' + n_z w'$ and $\tilde{V} = n_x \tilde{u} + n_y \tilde{v} + n_z \tilde{w}$. If the interface coincides with an inlet boundary, adding the velocity fluctuations as Eq. (13) would be equivalent to a Dirichlet boundary condition, where $\tilde{u}_i$ is the inlet mean flow. This method is denoted M1.

The second method is a volume source term [31] derived from an expansion of the implicit time discretization for the fluctuating velocity components u'_i at different time levels consistent with the 2nd-order difference scheme. The contribution to the momentum residuals reads

$$Q_i = \frac{\partial(\rho u'_i)}{\partial t}\Delta V \approx \frac{3(\rho u'_i)^{n+1} - 4(\rho u'_i)^n + (\rho u'_i)^{n-1}}{2\Delta t}\Delta V \tag{14}$$

where ΔV is the cell volume and Δt is the physical time step. The fluctuating velocity u'^{n+1}_i is taken from Eq. (2) but the values at previous times are computed as the predicted fluctuations, namely $u'^{n}_i = u^n_i - \langle u_i \rangle$ and $u'^{n-1}_i = u^{n-1}_i - \langle u_i \rangle$, respectively. This treatment prevents decoupling of the predicted flow solution from the target synthetic field, and adds the requirement of incorporating the time-averaged mean values $\langle u_i \rangle$ [31], which is computed as running-time average. Note that the contribution from Eq. (11) are added to the continuity, momentum and total energy equations, whereas the contribution from Eq. (14) are only added to the momentum equations. The turbulent fluctuations of other solution variables are expected to be reflected through the injection of velocity fluctuations. This method is denoted M2.

The third method introduces fluctuations by superimposing both previous methods. That is, the contribution from the source term given by Eq. (14) are added to the momentum equations. In addition, the contribution from the virtual flux term given by Eq. (11) is added to the continuity, momentum and total energy equations. This method is denoted M3.

B. Eddy Viscosity Treatment at Interface

A commutation error occurs in hybrid RANS-LES simulations since the hybrid filter width does not commute with the spatial derivative. Additional terms appears when computing the spatial derivative of a physical quantity f, as shown in Eq. (15)

$$\overline{\frac{\partial f}{\partial x_i}} = \frac{\partial \overline{f}}{\partial x_i} - \frac{\partial \Delta}{\partial x_i}\frac{\partial \overline{f}}{\partial \Delta} \tag{15}$$

where $\overline{(\cdot)}$ denotes filter operation. It has been shown that the commutation error (second term on RHS in Eq. (15)) can be large at RANS-LES interfaces [16]. The effects of adding the commutation term in hybrid RANS-LES simulations has been explored by Arvidson et al. [18] and by Davidson [17]. It was shown that by introducing commutation terms in the k and ω equations for a $k-\omega$ based hybrid model at zonal RANS-LES wall normal interfaces, the upstream RANS modeled kinetic energy levels could effectively be reduced to downstream SGS levels of modeled kinetic energy

without using any model dependent parameters. In this paper, the underlying RANS model considered is the SA-model which solves the transport equation for the modeled eddy viscosity $\tilde{\nu}$. Using Eq. (15), the commutation term for the convection term in the SA-model can be formulated as

$$\overline{\frac{\partial u_i \tilde{\nu}}{\partial x_i}} = \frac{\partial \overline{u}_i \tilde{\nu}}{\partial x_i} - \frac{\partial \Delta}{\partial x_i}\frac{\partial \overline{u}_i \tilde{\nu}}{\partial \Delta} \tag{16}$$

If one then considers a wall normal interface in the $x-$direction, the second term on the RHS in Eq. (16) can be disctretized as

$$\begin{aligned} S^c_{\tilde{\nu}} = \frac{\partial \Delta}{\partial x}\frac{\partial \overline{u}\tilde{\nu}}{\partial \Delta} &\approx \left(\frac{\Delta_{Hyb} - \Delta_{RANS}}{\Delta x}\right)\frac{\overline{u}_{RANS}\tilde{\nu}_{RANS} - \overline{u}_{Hyb}\tilde{\nu}_{Hyb}}{\Delta_{RANS} - \Delta_{Hyb}} \\ &= \frac{\overline{u}_{Hyb}\tilde{\nu}_{Hyb} - \overline{u}_{RANS}\tilde{\nu}_{RANS}}{\Delta x} \end{aligned} \tag{17}$$

where Δx is the length of the region in which the commutation terms are used for the $\tilde{\nu}_t$ equation. The RANS properties in Eq. (17) can either be taken from a precursor steady RANS simulation or upstream RANS values. The value of $\tilde{\nu}_{Hyb}$ is estimated from a Smagorinsky model expression [2]

$$\nu_{t,Hyb} = \min[(\kappa d)^2, (C_S\Delta)^2]S, \quad \nu_{t,Hyb} = f_{v1}\tilde{\nu}_{Hyb} \tag{18}$$

in order to provide a rapid transition form pure RANS levels of $\tilde{\nu}_t$, to a $\tilde{\nu}_t$-profile given by the hybrid length scale in Eq. (4). In Eq. (18), the modeling constant is set to $C_S = 0.2$, the length scale Δ is given by Eq. (5) and f_{v1} is the near-wall scaling function for the SA-model. The non-linear relationship between $\nu_{t,Hyb}$ and $\tilde{\nu}_{Hyb}$ is solved using a few iterations of a Newton-Rhapson solver.

The influence of the distance Δx, which is the length of the region in which the commutation terms are used in the equations for modeled turbulence, has been analyzed by Davidson [17], where he concluded that the larger the distance, the weaker the effect of the commutation terms. In this paper, Δx is taken as the characteristic cell size in the direction of the mean flow. For an unstructured code like M-Edge, Δx is approximated as the maximum edge length of the cell.

V. Results

The different injection methods defined in Section IV are evaluated in embedded hybrid RANS-LES simulations for developing turbulent plane channel flow and zero-pressure-gradient boundary layer. A set of cells coinciding with a plane defining the forcing-region are chosen manually, where the fluctuations from the STG in Eq. (2) are added by the methods defined by Eq. (13) (referred to as M1), Eq. (14) (referred to as M2) or the combination of both methods (referred to as M3).

The effect of the commutation term outlined in Section IV.B for the SA equation is evaluated for developing turbulent plane channel flow. The commutation given by Eq. (17) is added to the same cells where the fluctuations are added.

A. Turbulent channel flow at $Re_\tau = 5200$

Hybrid RANS-LES simulations of the turbulent flow in a plane channel are performed at $Re_\tau = 5200$. A hexahedral grid of dimensions $9\delta \times 2\delta \times 1.6\delta$ is discretized using $96 \times 96 \times 32$ cells. The resolution in wall units is set to $\Delta x^+ = 500$, $\Delta z^+ = 250$, and $\Delta y^+ \leq 1$ at the wall. Periodic boundary conditions are applied in the spanwise direction and adiabatic wall boundary conditions are used. Standard inlet and outlet boundary conditions are applied in the streamwise direction. The bulk Mach number M_b is set to 0.15. A baseline simulation is performed for a fully developed turbulent channel flow with periodic boundary condition in the streamwise direction using the SA-IDDES model which is used as reference. Emphasis will be put on how quickly the different methods outlined in Sections II and IV can re-establish fully developed turbulent conditions with the same grid and conditions. A precursor RANS simulation using the SA-model is used to generate initial conditions for the embedded simulation. Fluctuations are added at the interface at $\tilde{x}/\delta \approx 1.92$, where the IDDES is forced to be in RANS mode upstream of the interface. Reynolds stress statistics used by the STG are generated from the RANS SA-model using Eqs. (8) and (10).

The first test case evaluates the effect of the commutation term (17). The IDDES length scale in Eq. (4) is manipulated to work either in WMLES mode, by setting $f_{dt} = 1$, or by using the standard definition without any modification. Fluctuations are imposed at the interface using method M1. The effect of the commutation term is shown

in Figs. 2 -4. The response in friction velocity is shown in Fig. 2(a), and the velocity profile at 2δ downstream of the interface is shown in Fig. 2(b).

As can be observed in the Fig.2(a), the upstream RANS friction velocity deviates from the developed IDDES friction velocity, where the developed IDDES result underpredicts the target $u_\tau = 1$ by approximately 4%. This is due to a too short simulation domain in the spanwise direction, another developed IDDES simulation was performed with twice the domain size (3.2δ) in spanwise direction with the same resolution $\Delta z^+ = 250$, which yielded the desired value of $u_\tau = 1$ (not shown).

When the commutation term is applied, the IDDES is able to rapidly switch from RANS to hybrid mode, as the friction velocity reaches the developed results within 1δ and are almost spot on for the entire channel length. This is also achieved without forcing the IDDES to be in WMLES mode. The mean velocity profile agrees very well with the reference simulation after 2δ, as shown in Fig. 2(b). When no commutation term is applied, the results are different. If the IDDES is forced to be in WMLES mode, a longer adaption length is observed in the friction velocity, but are still within 5% after 1δ. When no commutation term is applied and not forcing the IDDES to be in WMLES, a slight over prediction of the friction velocity and an under prediction of the velocity profile is observed.

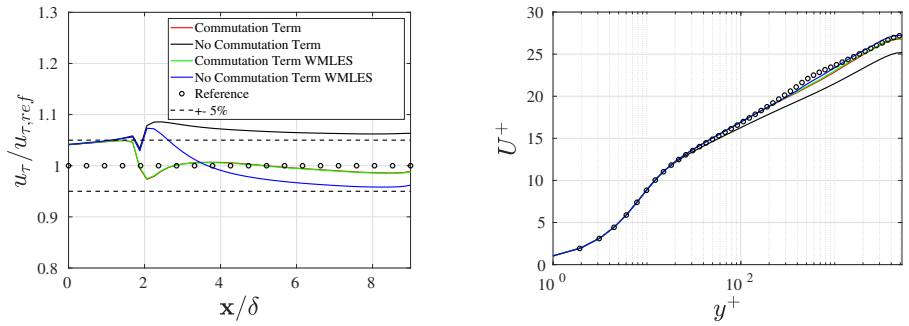

(a) Normalized friction velocity **(b) Mean velocity profile**

Fig. 2 Effect of commutation term applied at RANS-LES interface using M1 to inject fluctuations. Friction velocity and mean velocity profile for turbulent channel flow at $Re_\tau = 5200$. Velocity profile taken at 2δ downstream of interface. Green and red lines are on top of each other. Red and black lines are computed with no modification of l_{hyb} in Eq. (4), blue and green lines are computed with $f_{dt} = 1$ in the IDDES region.

The impact of the commutation term on the modeled eddy viscosity is shown in Fig. 3. A quick reduction of the turbulent viscosity is obtained across the interface due to the commutation term, where the reduced eddy viscosity levels reaches the downstream developed levels within 1δ. If no commutation term is applied, the IDDES has to be forced to WMLES mode in order to reduce the upstream RANS level viscosity. However, the reduction is relatively much slower compared to using the commutation term, where the fully developed levels are reached within 6δ. If no commutation term is applied and the model is not forced to be WMLES, the modeled eddy viscosity is not reduced at all across the interface, but rather slightly increased compared to the upstream RANS levels. The reason is that the excessive upstream RANS viscosity hinders the model to switch from the RANS length scale to the hybrid length scale, since f_{dt} remains unmodified across the interface. By using the commutation term, f_{dt} is modified implicitly with the reduced eddy viscosity, and can quickly switch to the hybrid length scale.

The positive impact of the commutation term is further verified in the response of the resolved shear stress (Fig. 4(a)) and resolved normal stresses (Fig. 4(b). When no commutation term is applied and without forcing the downstream domain to be in WMLES mode, most of the fluctuations from the STG are damped within 2δ. A slight difference is observed when using the commutation term for both zonal methods (i.e. setting f_{dt} to 1 in Eq. (6) or using the standard expression given by Eq. (4)), but both agree very well with the stresses from the reference simulation. When no commutation term is applied in the forced WMLES mode, a minor under prediction of the resolved stresses is observed.

In general, it is concluded that the positive response of using the commutation term at the wall-normal RANS-LES interface together with the synthetic fluctuations from the STG are large and greatly improves the transition from modeled RANS turbulence partly resolved turbulence in the downstream hybrid RANS-LES domain. Hence, the

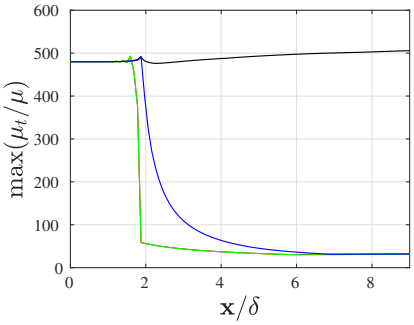

Fig. 3 Effect of commutation term applied at RANS-LES interface using M1 to inject fluctuations. Maximum turbulent eddy viscosity for turbulent channel flow at $Re_\tau = 5200$. Colors correspond to legend in Fig. 2(a). Green and red lines are on top of each other. Red and black lines are computed with no modification of l_{hyb} in Eq. (4), blue and green lines are computed with $f_{dt} = 1$ in the IDDES region.

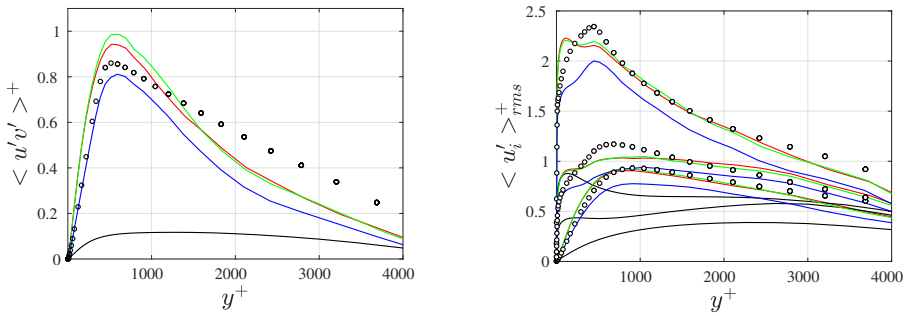

(a) Resolved shear stress

(b) RMS of resolved normal stresses

Fig. 4 Effect of commutation term applied at RANS-LES interface using M1 to inject fluctuations. Resolved shear stress and RMS of resolved normal stresses for turbulent channel flow at $Re_\tau = 5200$. Profiles are taken 2δ downstream of interface. Colors correspond to legend in Fig. 2(a). Red and black lines are computed with no modification of l_{hyb} in Eq. (4), blue and green lines are computed with $f_{dt} = 1$ in the IDDES region.

commutation term given by Eq. (17) for the $\tilde{\nu}_t$-equation is important and is used at the interface for the remaining test cases of this paper. f_{dt} is not forced to one but is computed from Eq. (6).

The second part to evaluate is considering the effects of imposing fluctuations at a wall-normal RANS-LES interface using the different injection methods (M1 - M3) outlined in Section IV.A. The results are shown in Figs. 5 and 6. Fig. 5(a) shows the response in friction velocity across the interface. All three methods experiences a sudden decrease in friction velocity across the interface, but remain within 5% for the entire downstream region. M2 experiences the largest decrease and does not reach the developed conditions. Closest to the reference simulation is M3, which is a superposition of the source term based on the time derivative and the virtual flux term based on the convective flux. The mean velocity profile shown in Fig. 5(b), where all methods show similar agreement with the reference simulation, measured 2δ downstream of the interface.

The effect of the different injection methods on the resolved stresses is shown in Fig. 6(a) and 6(b), where the profiles are measured 2δ downstream of the interface. A slight overestimation of the maximum value of resolved shear stress is observed for M1 and M3, but similar results are also reported in the work by Shur et al. [2], where the fluctutations are imposed at an inlet. M2 captures the near wall shear stress quite good but deviates more from the reference simulation further away from the wall. The same trends can be observed in the resolved normal stresses in Fig.

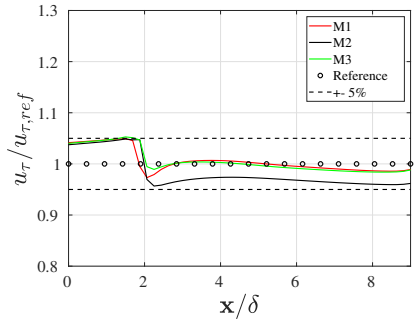

(a) Normalized friction velocity

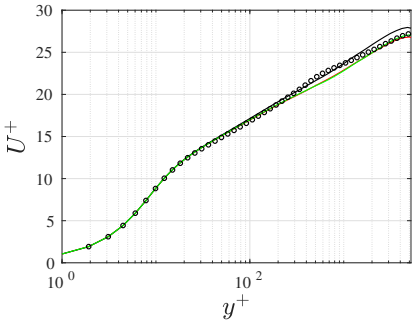

(b) Mean velocity profile

Fig. 5 Effect of different injection methods applied at RANS-LES interface. Friction velocity and mean velocity profile for turbulent channel flow at $Re_\tau = 5200$. Velocity profile taken at 2δ downstream of interface.

6(b), where M2 under predicts all normal stresses, M1 captures the streamwise stress very good and M3 gives a slight over estimation of the streamwise stress.

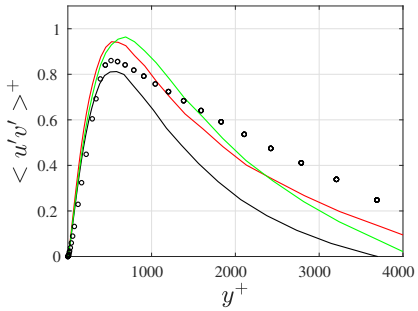

(a) Resolved shear stress

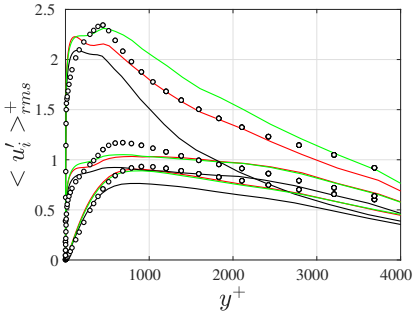

(b) RMS of resolved normal stresses

Fig. 6 Effect of different injection methods applied at RANS-LES interface. Resolved shear stress and RMS of resolved normal stresses for turbulent channel flow at $Re_\tau = 5200$. Profiles are taken 2δ downstream of interface. Colors correspond to legend in Fig. 5(a).

B. Zero-Pressure-Gradient Turbulent Boundary Layer at $Re_\theta \geq 3000$

The spatially developing zero-pressure-gradient (ZPG) turbulent boundary layer over a smooth flat plate is simulated using an zonal RANS-LES approach. The Reynolds number range covered by the simulation is approximately $3000 \leq Re_\theta \leq 6000$, where θ is the momentum thickness. The Mach number based on the free stream velocity is $M_0 = 0.2$. Profiles of u, v and ν_t from a precursor RANS simulation using the SA model is prescribed at the inlet boundary. An initial RANS region is prescribed by forcing $l_{hyb} = l_{RANS}$ in Eq. (4), and an embedded interface is prescribed at $x/\delta_0 = 4$, where δ_0 is the initial boundary layer thickness. Downstream of this interface, the IDDES length scale in Eq. (4) is unmodified. Synthetic turbulent fluctuations from the STG given by Eq. (2) and the commutation term given by Eq. (17) for the SA-model are imposed at the embedded interface to obtain a rapid development of downstream turbulence-resolving LES flow.

The grid used for the simulation is designed by Onera in the EU-FP7 Go4Hybrid and the Garteur AG54 projects. The dimensions of the computational domain in the streamwise, spanwise and in the wall-normal directions are, respectively,

$L_x = 113\delta_0$, $L_z = 5\delta_0$ and $L_y = 52\delta_0$. The computational domain is discretized using $587 \times 127 \times 103$ cells, which gives $7.8M$ cells. The wall units are $(\Delta x^+, \Delta y^+, \Delta z^+) = (100 - 200, 2, 50)$. Note that for $x/\delta_0 > 77$, grid cells are stretched in the streamwise direction in order to progressively damp the turbulent fluctuations. This procedure is common to ensure that the domain of interest is free from wave reflections from the outlet.

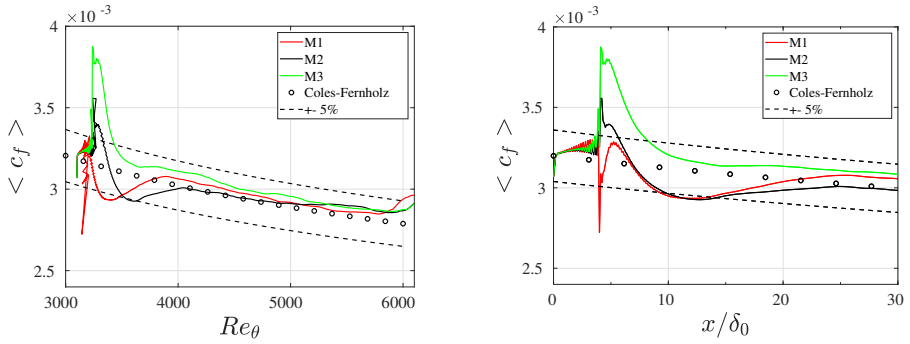

(a) $C_f(Re_\theta)$ **(b)** $C_f(x)$

Fig. 7 Effect of different injection methods applied at RANS-LES interface. Skin friction coefficient for ZPG boundary layer at $Re_\theta \geq 3000$. Results compared with Coles-Fernholz correlation [32].

The injection methods M1-M3 are assessed by imposing the fluctuations from the STG at the wall-normal RANS-LES interface. Fig. 7 shows the resulting skin friction coefficient in comparison with the Coles-Fernholz correlation [32]. Compared to results for the developing channel flow case 5(a), the methods show larger differences for this flow case. M1 gives a drop in the skin friction, a rapid increase and then a transition region to reach the correct trend according to the correlation after approximately $20\delta_0$ from the interface. On the other hand, M2 experiences a sudden increase across the interface, but shows a similar adaption trend as M2. M3 over estimates the skin friction initially but reaches developed flow conditions much quicker than the other two methods. The correct trend of M3 is reached after $7\delta_0$, a clear improvement compared to M1 and M2. However, it is important to highlight that all methods are within a 5% margin after $5\delta_0$ from the reference correlation, and give a correct decay of the skin friction further downstream in the boundary layer, as shown in Fig. 7(a).

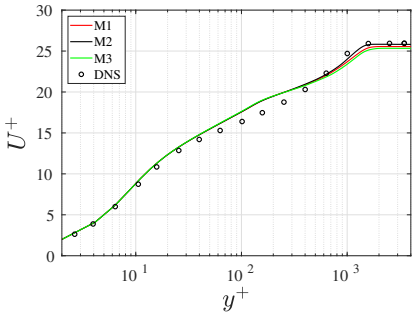

Fig. 8 Effect of different injection methods applied at RANS-LES interface. Mean velocity profile compared with DNS data [33] for ZPG boundary layer at $Re_\theta \geq 3000$.

The difference between the methods with respect to the mean velocity profile and resolved stresses measured at $Re_\theta = 4060$ are very small and yield similar small deviation from DNS [33], as shown in Figs. 8 and 9.

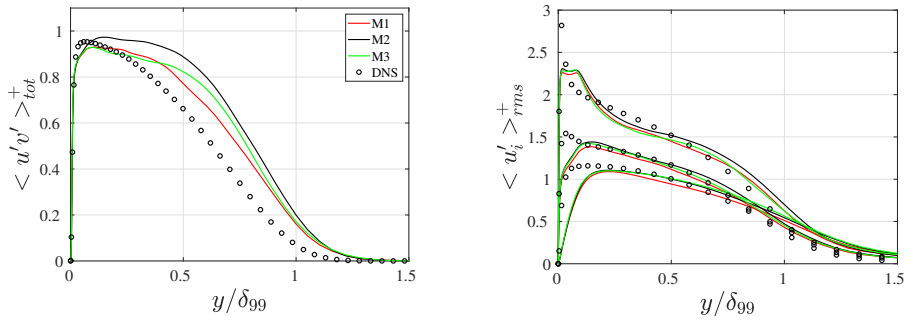

(a) Total shear stress **(b) RMS of resolved normal stresses**

Fig. 9 Effect of different injection methods applied at RANS-LES interface. Total shear stress and RMS of resolved normal stresses compared with DNS data [33] for ZPG boundary layer at $Re_\theta \geq 3000$.

VI. Summary and Conclusions

A sensitivity study on different formulations of synthetic turbulence has been conducted, which is imposed at the RANS-LES interface for zonal RANS-LES computations in order to mitigate the grey-area problem in the LES region, has been made in a compressible flow solver. Three injection methods have been implemented, where the synthetic turbulent fluctuations is numerically represented by means of, respectively, a volumetric source term, a virtual flux term, or a combination of thereof. The three methods were implemented by imposing the fluctuations (in the form of a source term, a flux term or a combination thereof) at an embedded wall-normal RANS-LES interface. Additionally, a formulation based on the commutation error for the convective term at the RANS-LES interface has been derived for the Spalart-Allmaras turbulence model, in order to reduce the modeled turbulent viscosity across the RANS-LES interface. This formulation is expressed as a source term, and is free from model dependent parameters. The three injection methods and the commutation term have been verified in embedded RANS-LES using SA-IDDES in a turbulent channel flow at $Re_\tau = 5200$ and zero-pressure-gradient boundary layer at $Re_\theta \geq 3000$.

The commutation term is able to effectively reduce the upstream RANS levels of turbulent viscosity to LES levels of turbulent viscosity across the embedded interface for the turbulent channel flow case. The transition occurs over a distance shorter than 1δ, where δ is the channel half width. The same effect can be achieved by forcing the IDDES to be in WMLES mode, however, this delays the transition length to above 4δ. If no commutation term is applied, or no explicit forcing of the IDDES to WMLES mode, the turbulent viscosity remains in RANS levels across the interface and dampens the fluctuations imposed by the STG, effectively driving the IDDES towards the RANS mode. Thus, it is concluded that the commutation term works very well and does not require any manual manipulation of the IDDES to force it to WMLES mode.

All the three injection methods perform very well for the turbulent channel flow case, where the virtual flux based method and the combination of the virtual flux term and the source term give nearly identical results. The two methods are able to reproduce reference simulation friction velocity within 1δ downstream from the interface. By using only the source term, the friction velocity does not fully recover for the downstream computational domain. The deviation is although very small (less than 5%) compared to the reference simulation.

In the simulation of the boundary layer flow, the discrepancy between the different injection methods are relatively large. The shortest recovery length with a well predicted skin friction level is produced by the combined flux and source term method. The other two approaches yield similar recovery lengths, considerably longer compared to the combined approach ($7\delta_0$ compared to $20\delta_0$, where δ_0 is the initial boundary layer thickness). However, all the simulations that are presented predict a skin friction distribution within 5% compared to the Coles-Fernholz correlation, which is used as a reference. Good agreement with DNS data further downstream is achieved for all simulation, with respect to mean velocity profile and resolved Reynolds stresses.

Acknowledgement

This work has been funded by the Swedish Governmental Agency for Innovation Systems (VINNOVA), the Swedish Defence Materiel Administration (FMV) and the Swedish Armed Forces within the National Aviation Research Programme (NFFP, Contract No. 2017–04887) and Saab Aeronautics. The simulations were performed on resources provided by the Swedish National Infrastructure for Computing (SNIC) at the Chalmers Centre for Computational Science and Computing (C3SE).

References

[1] Spalart, P., Jou, W.-H., Strelets, M., and Allmaras, S., "Comments on the Feasibility of LES for Wings, and on a Hybrid RANS/LES Approach," *Advanced in DNS/LES*, 1997.

[2] Shur, M. L., Spalart, P. R., Strelets, M. K., and Travin, A. K., "A hybrid RANS-LES approach with delayed-DES and wall-modelled LES capabilities," *International Journal of Heat and Fluid Flow*, Vol. 29, No. 6, 2008, pp. 1638 – 1649.

[3] Peng, S. H., "Hybrid RANS-LES modeling based on zero- and one-equation models for turbulent flow simulation," *4th International Symposium on Turbulence and Shear Flow Phenomena*, Vol. 3, 2005, pp. 1159–1164.

[4] Peng, S. H., "Hybrid RANS-LES modelling with an energy backscatter function incorporated in the LES mode," 2012, p. 9. https://doi.org/10.1615/ICHMT.2012.ProcSevIntSympTurbHeatTransfPal.260.

[5] Girimaji, S. S., and Wallin, S., "Closure modeling in bridging regions of variable-resolution (VR) turbulence computations," *Journal of Turbulence*, Vol. 14, No. 1, 2013, pp. 72–98. https://doi.org/10.1080/14685248.2012.754893.

[6] Batten, P., Goldberg, U., and Chakravarthy, S., "Interfacing Statistical Turbulence Closures with Large-Eddy Simulation," *AIAA Journal*, Vol. 42, No. 3, 2004, pp. 485–492. https://doi.org/10.2514/1.3496.

[7] Davidson, L., and Billson, M., "Hybrid LES-RANS using synthesized turbulent fluctuations for forcing in the interface region," *International Journal of Heat and Fluid Flow*, Vol. 27, 2006, pp. 1028–1042.

[8] Shur, M., Spalart, P., Strelets, M., and Travin, A., "Synthetic Turbulence Gnerators for RANS-LES Interfaces in Zonal Simulations of Aerodynamic and Aeroacoustic Problems," *Flow, Turbulence and Combustion*, Vol. 93, 2014, pp. 63–92.

[9] Jarrin, N., Benhamadouche, S., Laurance, D., and Prosser, R., "A synthetic-eddy-method for generating inflow conditions for large-eddy simulations," *International Journal of Heat and Fluid Flow*, Vol. 27, 2006, pp. 585–593.

[10] Jarrin, N., Prosser, R., Uribe, J.-C., Benhamadouche, S., and Laurance, D., "Reconstruction of turbulent fluctuations for hybrid RANS/LES simulations using a Synthetic-Eddy Method," *International Journal of Heat and Fluid Flow*, Vol. 30, 2009, pp. 435–442.

[11] Poletto, R., Revell, A., Craft, T., and Jarrin, N., "Divergence free synthetic eddy method for embedded LES inflow boundary conditions," *Seventh international Symposium On Turbulence and Shear Flow Phenomena (TSFP-7)*, 2011.

[12] Mathey, F., "Aerodynamic noise simulation of the flow past an airfoil trailing-edge using a hybrid zonal RANS-LES," *Computers & Fluids*, Vol. 37, 2007, pp. 836–843.

[13] Davidson, L., "Zonal PANS: evaluation of different treatments of the RANS–LES interface," *Journal of Turbulence*, Vol. 17, No. 3, 2016, pp. 274–307.

[14] Schmidt, S., and Breuer, M., "Source term based synthetic turbulence inflow generator for eddy-resolving predictions of an airfoil flow including a laminar separation bubble," *Computer & Fluids*, Vol. 146, 2017, pp. 1–22.

[15] Probst, A., "Scale-Resolving Simulations on Unstructured Meshes with a Low-Dissipation Low-Dispersion Scheme," *New Results in Numerical and Experimental Fluid Mechanics XI*, Springer International Publishing, Cham, 2018, pp. 489–498.

[16] Hamba, F., "Analysis of filtered Navier–Stokes equation for hybrid RANS/LES simulation," *Physics of Fluids*, Vol. 23, No. 1, 2011, p. 015108.

[17] Davidson, L., "Two-equation hybrid RANS–LES models: a novel way to treat k and at inlets and at embedded interfaces," *Journal of Turbulence*, Vol. 18, No. 4, 2017, pp. 291–315.

[18] Arvidson, S., Davidson, L., and Peng, S.-H., "Interface methods for grey-area mitigation in turbulence-resolving hybrid RANS-LES," *International Journal of Heat and Fluid Flow*, Vol. 73, 2018, pp. 236–257.

[19] Aupoix, B., and Spalart, P., "Extensions of the Spalart–Allmaras turbulence model to account for wall roughness," *International Journal of Heat and Fluid Flow*, Vol. 24, No. 4, 2003, pp. 454–462. Selected Papers from the Fifth International Conference on Engineering Turbulence Modelling and Measurements.

[20] Eliasson, P., "Edge, a Navier–Stokes solver for unstructured grids," *Finite Volumes for Complex Applications*, CP849, Vol. III, 2002, pp. 527–534.

[21] Eliasson, P., Eriksson, S., and Nordström, J., "The influence of weak and strong solid wall boundary conditions on the convergence to steady-state of the navier-stokes equations," *AIAA Paper*, , No. 2009-3551, 2009.

[22] Probst, A., and Ströer, P., "Comparative Assessment of Synthetic Turbulence Methods in an Unstructured Compressible Flow Solver," *Progress in Hybrid RANS-LES Modelling*, edited by Y. Hoarau, S.-H. Peng, D. Schwamborn, A. Revell, and C. Mockett, Springer International Publishing, Cham, 2020, pp. 193–202.

[23] Rung, T., Bunge, U., Schatz, M., and Thiele, F., "Restatement of the Spalart-Allmaras Eddy-Viscosity Model in Strain-Adaptive Formulation," *AIAA Journal*, Vol. 41, No. 7, 2003, pp. 1396–1399. https://doi.org/10.2514/2.2089.

[24] Laraufie, R., and Deck, S., "Assessment of Reynolds stresses tensor reconstruction methods for synthetic turbulent inflow conditions. Application to hybrid RANS/LES methods," *International Journal of Heat and Fluid Flow*, Vol. 42, 2013, pp. 68–78.

[25] Wallin, S., and Johansson, A. V., "An explicit algebraic Reynolds stress model for incompressible and compressible turbulent flows," *Journal of Fluid Mechanics*, Vol. 403, 2000, p. 89–132. https://doi.org/10.1017/S0022112099007004.

[26] Wilcox, D., *Turbulence Modeling for CFD (Third Edition)*, 2006.

[27] Eliasson, P., and Weinerfelt, P., "Recent applications of the flow solver Edge," *7th Asian CFD Conference*, 2007.

[28] Jameson, A., "Time-dependent calculations using multigrid with applications to unsteady flows past airfoils and wings," *AIAA Paper*, , No. 91-1596, 1991.

[29] Löwe, J., Probst, A., Knopp, T., and Kessler, R., "Low-Dissipation Low-Dispersion Second-Order Scheme for Unstructured Finite-Volume Flow Solvers," *AIAA Journal*, Vol. 54, 2016. https://doi.org/10.2514/1.J054956.

[30] Carlsson, M., Davidson, L., Peng, S., and Arvidson, S., "Parametric Investigation of Low-dissipation Low-dispersion Schemes for Unstructured Flow Solvers in Large Eddy Simulation," *2020 AIAA SciTech*, 2020.

[31] Probst, A., "Implementation and assesment of the Synthetic-Eddy Method in an unstructured compressible flow solver," *Progress in Hybrid RANS-LES Modelling. NNFMMD*, Vol. 137, 2018, pp. 91–101.

[32] Nagib, H. M., Chauhan, K. A., and Monkewitz, P. A., "Approach to an asymptotic state for zero pressure gradient turbulent boundary layers," *Philosophical Transactions of the Royal Society A: Mathematical, Physical and Engineering Sciences*, Vol. 365, No. 1852, 2007, pp. 755–770.

[33] Schlatter, P., and Örlü, R., "Assessment of direct numerical simulation data of turbulent boundary layers," *Journal of Fluid Mechanics*, Vol. 659, 2010, pp. 116 – 126.